Applied Surface Science 320 (2014) 871–882

Contents lists available at ScienceDirect

Applied Surface Science

journal homepage: www.elsevier.com/locate/apsusc

# Extracellular matrix inspired surface functionalization with heparin, fibronectin and VEGF provides an anticoagulant and endothelialization supporting microenvironment

Xue Wang[a], Tao Liu[a,b], Yuan Chen[a], Kun Zhang[a,c], Manfred F. Maitz[a,d], Changjiang Pan[b], Junying Chen[a,*], Nan Huang[a]

[a] Key Laboratory of Advanced Technology for Materials of Chinese Education Ministry, School of Materials Science and Engineering, Southwest Jiaotong University, Chengdu, PR China
[b] Jiangsu Provincial Key Laboratory for Interventional Medical Devices, Huaiyin Institute of Technology, Huai'an, PR China
[c] School of Life Science, Zhengzhou University, Zhengzhou, PR China
[d] Leibniz Institute of Polymer Research Dresden, Max Bergmann Center of Biomaterials, Hohe Str. 06, 01069 Dresden, Germany

ARTICLE INFO

*Article history:*
Received 18 April 2014
Received in revised form 27 August 2014
Accepted 2 September 2014
Available online 8 September 2014

*Keywords:*
Heparin
Fibronectin
VEGF
Anticoagulant
Endothelialization

ABSTRACT

The biocompatibility of currently used coronary artery stent is still far from perfect, which closely related to insufficient endothelialization and thrombus formation. In this study, heparin, fibronectin and VEGF were immobilized on Ti surface to construct a multifunctional microenvironment with favorable properties to inhibit thrombosis formation and promote endothelialization simultaneously. The microenvironment on Ti surface was characterized in detail and demonstrated that the Hep/Fn/VEGF biofunctional coating was constructed successfully on Ti surface. The influence of surface properties such as chemical composition, roughness, hydrophilicity, and binding density of biomolecules on the performances of hemocompatibility and cytocompatibility was evaluated and discussed. Modified surface significantly enhanced the AT III binding density and prolonged the clotting time. In vitro platelet adhesion and activation assays further proved that the modified surface presented favorable anticoagulant property. In addition, the proliferation of endothelial progenitor cells (EPCs) and endothelial cells (ECs) on the Hep/Fn/VEGF biofunctional coating was significantly promoted. In conclusion, the Hep/Fn/VEGF biofunctional coating was successfully constructed with desirable anticoagulant and endothelialization supporting properties. This work may provide a promising approach for biofunctional surface modification of coronary artery stent to acquire a desired multifunctional microenvironment.


## 1. Introduction

Cardiovascular diseases have been the leading cause of disability and mortality in modern society. In the western world, there are more than 50% of patients with coronary artery disease (CAD) who require percutaneous transluminal coronary angioplasty (PTCA) annually [1,2]. These blood-contacting biomedical devices benefit millions of patients. However, a significant number of patients (up to 20–30%) develop restenosis 3–6 months after the PTCA operation [3–6]. In stent restenosis is attributed to mechanical injury caused during the operation that subsequently leads to endothelial cell dysfunction, thrombosis at the site of injury and smooth muscle cells (SMCs) proliferation and migration. These processes contribute to neointima formation and in stent restenosis [7–9]. Hemocompatibility of blood-contacting biomedical devices therefore is very important for their long-term implantation. Now, it is generally accepted that a confluent layer of endothelial cells (ECs) is the best surface to prevent adverse cardiac events. Delayed or insufficient endothelialization is considered as a key factor of late-thrombosis and restenosis. Therefore, rapid in situ re-endothelialization after cardiovascular devices implantation is urgently required. Nowadays, a focus is made on the implantation of biofunctional materials that capture endothelial progenitor cells (EPCs) from blood and induce differentiation to autologous ECs. Numerous studies have demonstrated that EPCs can differentiate to ECs under the inducement of specific growth factors

* Corresponding author at: School of Material Science and Engineering, Southwest Jiaotong University, Chengdu 610031, PR China. Tel.: +86 28 87634148; fax: +86 28 87600625.
*E-mail address:* chenjy@263.net (J. Chen).

http://dx.doi.org/10.1016/j.apsusc.2014.09.004
0169-4332/

and chemokines [10–12]. Thereby, induction of EPCs homing and adhesion may facilitate rapid endothelialization on the surface of implanted biomaterials.

A variety of materials have been applied to improve the biocompatibility of cardiovascular devices, including alloys and ceramic coatings [13], such as Ti-$O_{2-x}$ coating [14] and DLC films [15], and polymer coatings [16]. Of these biomaterials, titanium (Ti) has been extensively used for several years due to its excellent mechanical properties, corrosion resistance, and particularly favorable biocompatibility [17]. However, for clinical applications, the long-term biological interaction between the implant and the surrounding tissues remains critical. Recently, numerous studies have suggested that surface-immobilization of specific biomolecules to mimetic the native microenvironment of blood vessels would provide favorable anticoagulant and induced-endothelialization properties for biomedical devices [5]. Numerous functional biomolecules, such as heparin [18], chitosan [19], tropoelastin [20], RGD peptides [21], anti-CD34 antibody [22], and extracellular matrix proteins [23,24] have being studied in surface biofunctional modification. Depending on the selected biomolecules, the modified surface will acquire favorable hemocompatibility [25,26] or cytocompatibility [27,28]. However, up to now, many studies have focused on improving only one aspect of biocompatibility, and few studies have simultaneously explored the hemocompatibility and re-endothelialization. In most cases, although the hemocompatibility of biomaterials is improved with anticoagulant biomolecules, the modified surface suppresses ECs adhesion and proliferation. In contrast, when ECs growth is significantly promoted by adhesive biomolecules, such as extracellular matrix proteins, the surface also becomes pro-thrombogenic. There seems to be a conflict between anticoagulation and re-endothelialization [29,30]. Co-immobilization of specific biomolecules on an implant may combine the properties of each individual biomolecule, which may help overcome the contradiction between anticoagulation and re-endothelialization.

For this purpose, heparin (Hep), fibronectin (Fn), and vascular endothelial growth factor (VEGF) were chosen as the constituents for surface modification in the present study. Heparin is a widely used anticoagulant in the clinical treatment of venous thromboembolism and acute coronary syndromes [31]. It interacts with antithrombin III (AT III) and promotes AT III-mediated inhibition of the coagulation pathway by increasing the affinity of AT III to thrombin [32]. Heparin can also suppress SMCs adhesion and proliferation [33]. Moreover, the activity of heparin binding growth factors can be enhanced by interaction with heparin [34]. Fn as one of the most important ECM proteins produced by ECs, SMCs, and fibroblasts consists of two monomers linked by a disulfide bond at their C termini [23]. Fn possesses multiple binding domains to interact with ECM proteins, cell surface integrins, and growth factors [35]. In particular, Fn can interact with the specific integrins α5β1 and αvβ3 expressed on ECs, and thereby promotes cell adhesion and migration [36]. However, Fn is also reported to participate in platelet adhesion and aggregation through the integrin aIIbβ3 receptors on the platelet membrane [37]. Therefore, surface modification of blood contacting materials by Fn only is not suitable, but complexes of heparin and Fn may change their individual properties, which result in an improved hemocompatibility and support of ECs and EPCs adhesion [38,39]. Besides, heparin is a highly acidic molecule, whereas the isoelectric point of Fn is at ~5.5. Therefore, under weak acidic conditions an electrostatic Hep/Fn complex can be formed. VEGF is one of the most potent and widely used key regulators of ECs survival, EPCs differentiation and new blood vessel formation [40–43]. VEGF has five isomers, namely VEGF121, 165, 183, 189, and 206, which exhibit differences in their amino acids and heparin binding sites. Among these, VEGF 165 possesses the best heparin binding activity and simulates ECs growth.

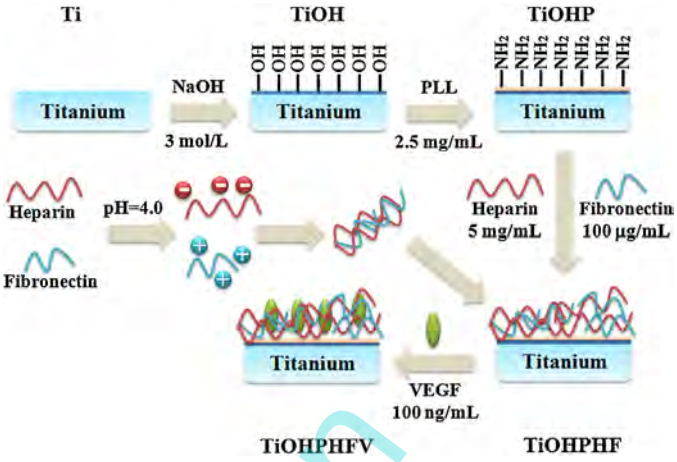


**Fig. 1.** Sketch of Hep/Fn/VEGF biofunctional coating on Ti substrate.

In this study, Hep/Fn complex was prepared under acidic conditions according to our previous investigations [38,39] and electrostatically assembled to an NaOH activated Ti surface, with the aim of construct a multifunctional microenvironment with favorable properties to inhibit thrombosis formation and promote endothelialization simultaneously. VEGF was further introduced to the surface via specific interaction with heparin to induce EPCs adhesion and proliferation. In this work, taking the influence of surface physicochemical properties into consideration, we expect the Hep/Fn/VEGF modified surface can selectively inhibit platelets adhesion and activation and promote ECs and EPCs proliferation.

## 2. Materials and methods

### 2.1. Reagents

Ti substrates (99.5% purity, Baoji, China, Ø 10 mm) were mirror-polished and ultrasonically cleaned three times successively with acetone, absolute alcohol and deionized water ($dH_2O$) for 5 min each and then dried. 0.1 M phosphate buffered saline (PBS, pH 7.4) was purchased from Hyclone Co. Ltd., and adjusted to pH 4 when used as the solvent of heparin and Fn solution. Low molecular weight heparin (≥160 U/mg) was purchased from Shanghai Bioscience and technology. Fn (from human), VEGF-A (from human), Poly-l-lysine (PLL, MW 150,000–300,000), Toluidine Blue O (TBO), Acid Orange II (AO II), rhodamine 123, 4′,6-diamidino-2-phenylindole (DAPI) and mouse monoclonal anti-human p-selectin antibody were purchased from Sigma–Aldrich. Mouse polyclonal antihuman Fn antibody, mouse monoclonal anti-human AT III antibody, horseradish peroxidase (HRP) conjugated goat anti-mouse IgG antibody and TMB (3,3′,5,5′-tetramethylbenzidene) for the immunochemistry tests, F12, DMEM culture medium for cells culture and proliferation test were purchased from BD Biosciences, San Jose, CA. Activated partial thromboplastin time (APTT) kits for coagulation time test were purchased from Sunbio, China. Fluorescein isothiocyanate (FITC)-conjugated rabbit anti human VEGF antibody and FITC-conjugated goat anti-mouse IgG antibody were purchased from Boster Biological Technology (Wuhan, China). All the other reagents used in the experiments were of the highest analytical purity (>99.9%).

### 2.2. Preparation of Hep/Fn/VEGF biofunctional coatings on Ti

The fabrication process of Hep/Fn/VEGF biofunctional coating on Ti substrate is schematically shown in Fig. 1. First, Ti substrates were activated by 3 M NaOH solution at 80 °C for 12 h to produce

**Table 1**
Explanation of the samples.

| Sample ID | Preparation of the samples |
|---|---|
| Ti | Pristine titanium |
| TiOH | Pristine Ti activated by 3 M NaOH |
| TiOHP | TiOH amine by 2.5 mg/mL PLL |
| TiOHPH | TiOHP interacted with 2.5 mg/mL heparin |
| TiOHPF | TiOHP interacted with 50 μg/mL fibronectin |
| TiOHPHF | TiOHP interacted with equal volume of 5 mg/mL heparin (pH 4) and 100 μg/mL fibronectin (pH 4) mixture |
| TiOHPHFV | TiOHPHF interacted with 100 ng/mL VEGF |

a negatively charged super hydrophilic surface, and then the samples were boiled with $dH_2O$ at 80 °C for 12 h to remove the residual NaOH. Second, above samples were immersed in 2.5 mg/mL PLL solution and reacted at 4 °C for 12 h to obtain an amino-rich surface. Third, equal volume of 5 mg/mL heparin (pH 4) and 100 μg/mL Fn (pH 4) were mixed and blended thoroughly at 37 °C for 1 h, and then the PLL coated samples were subsequently immersed in Hep/Fn mixture and reacted at 37 °C for 3 h; in addition, samples reacted alone with 2.5 mg/mL heparin or 50 μg/mL Fn were used as control. Thereafter, 50 μL of VEGF solution (100 ng/mL) was added to Hep/Fn immobilized surface and incubated at 37 °C for 2 h. Each step before interacting with biomolecules, the samples was rinsed with $dH_2O$ to remove the unattached biomolecules. The explanation of different samples was listed in Table 1.

### 2.3. Qualitative characterization of Hep/Fn/VEGF biofunctional coating

#### 2.3.1. XPS

The surface chemical compositions of the samples were determined by standardized X-ray photoelectron spectroscopy (XPS) measurement on an AXIS His spectrometer with a monochromatic A1 $K_\alpha$ X-ray source (1486.6 eV photons, 150 W). The chamber pressure was below $2 \times 10^{-9}$ Torr. The binding energy scale was calibrated by setting the $C_{1s}$ peak at 284.6 eV.

#### 2.3.2. AFM

The surface topography and the roughness before and after Hep/Fn/VEGF immobilization were characterized by an Atomic force microscope (AFM) in tapping mode [44]. AFM was performed at room temperature and the image analysis was processed by CSPM Imager software.

#### 2.3.3. Water contact angle measurement

A contact angle apparatus (JY-82, China) with a horizontal microscope was used for measuring the static water contact angle on samples surface. The test was performed at room temperature and the contact angle was calculated by a circle segment function of the DSA 1.8 software.

#### 2.3.4. VEGF immunofluorescence staining

Immunofluorescence staining was used to qualitative characterize the immobilized VEGF on samples surface. In brief, the samples were firstly fixed with 2.5% glutaraldehyde in PBS for 2–4 h and then blocked with 1 wt% bovine serum albumin (BSA) at 37 °C for 30 min. Subsequently, the samples were rinsed three times with PBS and then 50 μL fluorescein isothiocyanate (FITC) conjugated rabbit anti-human VEGF antibody (1/100 dilution in PBS) was added to samples surface and incubated at 37 °C for 30 min in dark. After rinsing with PBS, the samples were observed and photographed by a fluorescence microscope (DMRX, Leica, Germany).

### 2.4. Quantitative characterization of Hep/Fn/VEGF biofunctional coating

#### 2.4.1. Heparin quantification

The amount of immobilized heparin on the samples was measured using the TBO assay. In brief, the samples were incubated in 5 mL TBO solution (0.04 wt% TBO in 0.01 M HC1/0.2 wt% NaC1) at 37 °C for 4 h in order that the Hep/TBO complex was formed on the samples surfaces. Then the samples were thoroughly rinsed with $dH_2O$ three times and immersed in 5 mL of 80% ethanol/0.1 M NaOH (v/v: 4/1) solution to dissolve the Hep/TBO complex. Subsequently, the extinction of above eluate was determined in a microplate reader (Quant, Bio-tek instruments Inc.) at 530 nm wavelength. The amount of immobilized heparin on different samples surface were calculated according to a calibration standard curve.

The calibration curve was prepared as following: equal volume of 0.04 wt% TBO was firstly added to a known concentration of heparin solution and incubated at 37 °C for 4 h. Then the mixture was centrifuged at 3500 rpm for 10 min, and the Hep/TBO precipitate was dissolved in 5 mL of 80% ethanol/0.1 M NaOH (v/v: 4/1) thoroughly.

#### 2.4.2. Semi-quantitative determination of fibronectin

The amount of immobilized Fn on samples surface was determined by semi-quantitative immunochemistry. The process was described as following: the samples were firstly blocked with 1 wt% BSA and rinsed three times with PBS. Then 20 μL mouse monoclonal anti-human Fn antibody (1/250 dilution in PBS) was added to the samples surface and incubated at 37 °C for 1 h. After PBS rinsing, 20 μL horseradish peroxidase (HRP) conjugated goat anti-mouse IgG antibody (1/100 dilution in PBS) was added to samples surface and incubated at 37 °C for 1 h. Thereafter, the samples were rinsed three times again with PBS and 120 μL TMB was added to the samples surface and incubated in dark for 10 min, 50 μL 1 M $H_2SO_4$ was subsequently added to stop the peroxidase catalyzed reaction. Ultimately, 120 μL reacting solution was transferred from each samples surface into a 96-well plate and determined in a microplate reader at 450 nm wavelength.

### 2.5. Hemocompatibility evaluation of Hep/Fn/VEGF biofunctional coating

#### 2.5.1. AT III binding to heparin

The amount of absorbed AT III on the samples surface was measured semi-quantitatively by immunochemistry. For preparation, fresh human whole citrate anticoagulated blood was centrifuged at 3000 rpm for 15 min to obtain platelet-poor plasma (PPP). Then 50 μL PPP was added to samples surface and incubated at 37 °C for 15 min. The following detecting process was similar with the procedure of Fn semi-quantitative characterization except for the type of used antibody, here, mouse anti-goat antibody (1/200 dilution in PBS) and HRP conjugated goat anti-rabbit polyclonal antibody (1/200 dilution in PBS) were used as first antibody and second antibody, respectively.

#### 2.5.2. Clotting time assay

The activated partial thromboplastin time (APTT) was used to evaluate the influence of heparinized surface on the intrinsic coagulation system. Briefly, the samples were first immersed in 350 μL PPP and incubated at 37 °C for 30 min. Then, 300 μL incubated PPP from each sample was transferred to the test tube. Finally, the coagulation time was evaluated by a clotting time analyzer (ACL-200, Beckman Coulter, USA).

For prothrombin time (PT) and thrombin time (TT) assay, 100 μL PT or TT reagent was firstly mixed with 100 μL incubated PPP and

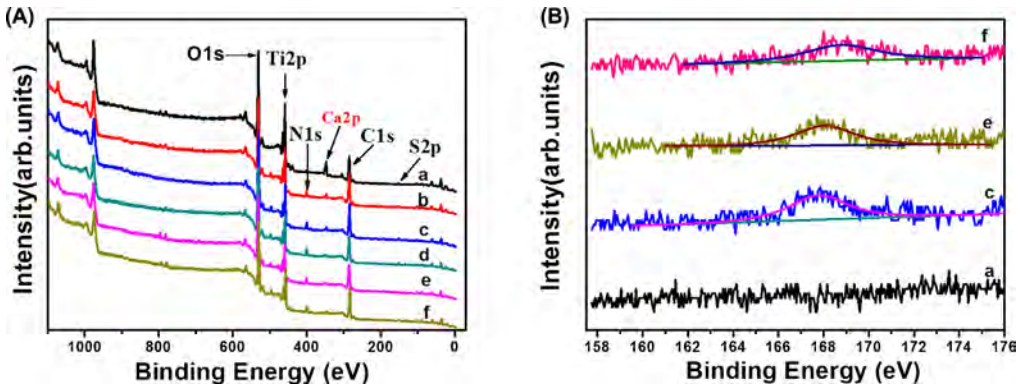


**Fig. 2.** (A) XPS full spectrum and (B) sulfur high resolution spectrum of (a) TiOH; (b) TiOHP; (c) TiOHPH; (d) TiOHPF; (e) TiOHPHF; (f) TiOHPHFV.

incubated at 37 °C for 30 min, subsequently the clotting time was measured using the clotting time analyzer.

*2.5.3. Platelet analysis*

In vitro platelet adhesion was used to determine amount, morphology and aggregation of the adherent platelets on different samples. First, fresh human whole citrate anticoagulated blood was centrifuged at 1500 rpm for 15 min to obtain platelet-rich plasma (PRP), and 50 μL PRP was added on samples surface and incubated at 37 °C for 1 h. Then the samples were rinsed 3 times with PBS and fixed in 2.5% glutaraldehyde for 12 h at room temperature. Thereafter, the samples were inspected by scanning electron microscopy (SEM, Philips Quanta 200) after standard dehydration and dealcoholization. LDH test was used to detect the amount of adherent platelets. Briefly, 50 μL PRP was added to samples surface and incubated at 37 °C for 1 h. After rinsing with PBS, 40 μL 1% Triton-X 100 was added to each sample and incubated 5 min at 37 °C. Subsequently, 25 μL lysate was transferred from the surfaces into a 96-well plate and 200 μL chromogenic agent (10 mg/mL Pyr and 10 mg/mL NADH powder dissolved in Tris base buffer) was added before test. The absorbance of different samples was recorded in a microplate reader at 340 nm wavelength.

P-selectin was quantified by immunochemistry to evaluate the activation degree of adherent platelets on different samples surface. The method was similar to AT III binding assay, and the only different was that the first antibody was mouse anti-human p-selectin monoclonal antibody.

*2.6. Cellular compatibility evaluation of Hep/Fn/VEGF biofunctional coating*

*2.6.1. EPCs, ECs culture and seeding*

EPCs were isolated from femur and tibia bone marrow of Sprague-Dawley (SD) rat. The bone marrow was firstly extracted and flushed into suspension with α-Modified Eagle's Medium (α-MEM) containing 10% fetal bovine serum (FBS), the suspended cells were then transferred into a culture flask and cultivated in incubator at 37 °C under 5% $CO_2$ [45]. Subculture was performed when confluency was more than 80%. The cells were digested and subcultured 2–3 times in one week and the pure bone stem cells (BMSCs) were obtained. Then, BMSCs were cultivated in α-MEM containing 10% FBS and 10 ng/mL VEGF, and subcultured for about 3–4 times to acquire EPCs. Finally, cells were designated as EPCs based on the identification of morphology and specific markers.

ECs were isolated from human umbilical vein by collagenase digestion method and cultivated in Dulbecco's Modified Eagle Medium/F12 (DMEM/F12) containing 20% FBS, 20 μg/mL endothelial cell growth supplement (ECGS) and 2 μmol/L glutamine (Gln). After 24 h, the culture medium was removed and the cells were rinsed with 0.9% NaCl to remove the residual blood cells, and then fresh medium were added. Before use, the medium was renewed every two days.

Prior to seeding the cells, all the pristine Ti and TiOH samples were sterilized by autoclavation at 120 °C for 30 min. The PLL solution, heparin solution, Fn solution and VEGF solution were sterile-filtered. The TiOHP, TiOHPH, TiOHPF, TiOHPHF, TiOHPHFV samples were prepared under aseptic conditions. Then EPCs, ECs were seeded on the samples surface at a density of $5 \times 10^4$ cells/mL and incubated at 37 °C under 5% $CO_2$ for 1 day and 3 days.

*2.6.2. EPCs, ECs proliferation assay and fluorescence staining*

The cell proliferation ability on different sample surfaces was evaluated by calculating cells number after 1 and 3 days culture, respectively. Fluorescence staining was used to observe the morphology of EPCs or ECs on different samples surface. Briefly, after cell culture, the samples were rinsed three times with PBS, and then fixed in 2.5% glutaraldehyde for 12 h at room temperature. After rinsing with PBS, rhodamine 123 was subsequently added to each sample surface and incubated at 37 °C for 20 min under dark condition. Thereafter, the samples were rinsed three times with PBS and observed by fluorescence microscopy.

*2.7. Statistical analysis*

At least three independent experiments and four parallel samples were performed for the assays described above. The data was analyzed with the SPSS 11.5 software and expressed as mean ± standard deviation (SD). The statistical difference analysis was performed by the origin 8.0 software. The probability values $p < 0.05$ were considered to indicate significant differences statistically ($^{*}p < 0.05$, $^{**}p < 0.01$, $^{***}p < 0.001$).

## 3. Results

*3.1. Qualitative characterization results of Hep/Fn/VEGF biofunctional coating*

*3.1.1. XPS*

XPS was used to characterize the alteration of surface chemical composition during biomolecules immobilization. The XPS spectra of different samples with the element peaks indicated is shown in Fig. 2A. Ca2p peaks (~346.9 eV) appeared probably due to the contamination during NaOH activation, because the NaOH reagent used in this study contains trace amounts of calcium salt. Compared with TiOH samples, Ti2p peaks (~460 eV) decreased and new N1s peaks (~400 eV) appeared on TiOHP samples. High resolution sulphur (in Fig. 2B) shows that sulphur appeared on TiOHPH, TiOHPHF and TiOHPHFV compared with TiOH samples. In combination with

**Table 2**
Elemental composition of different samples surface determined by XPS.

| Sample ID | C% | N% | O% | S% |
|---|---|---|---|---|
| TiOH | 42.7 ± 1.1 | 0.1 ± 0.02 | 57.2 ± 1.1 | 0 |
| TiOHP | 52.0 ± 1.6 | 5.5 ± 0.5 | 42.5 ± 2.1 | 0 |
| TiOHPH | 50.8 ± 1.1 | 5.4 ± 0.6 | 42.7 ± 0.9 | 1.1 ± 0.2 |
| TiOHPHF | 46.8 ± 2.8 | 6.6 ± 0.7 | 45.8 ± 3.1 | 0.8 ± 0.1 |
| TiOHPHFV | 51.4 ± 1.1 | 6.8 ± 0.5 | 41.2 ± 1.5 | 0.6 ± 0.06 |

the chemical elemental semi-quantitative results that are listed in Table 2, it can be concluded that nitrogen appeared on TiOHP samples and the nitrogen content increased on TiOHPH, TiOHPHF and TiOHPHF samples compared with TiOHP, and each is different. What is more, sulphur appeared on TiOHPH, TiOHPHF and TiOHPHFV samples but the content decreased successively (Table 2). This result indicated the heparin was successfully immobilized on PLL coated surface, and the VEGF binding may block the exposure of heparin and thereby cause the decreasing of sulphur content. Moreover, the increasing of nitrogen content may indicated the success immobilization of Fn and VEGF, but specific analysis of the quantity and activity of the biomolecules is mandatory.

### 3.1.2. AFM

Surface morphology and roughness of different samples were investigated by AFM. As shown in Fig. 3A and Table 3, pristine Ti surface presents a flat and smooth morphology, with an average roughness of Ra = 3.65 ± 0.27 nm. After NaOH activation, the roughness increased to Ra = 38 ± 1.51 nm and presented a uniform taper-pointed granules forming morphology, which has been demonstrated composed of micron and submicron pores [46]. The surface roughness after heparin, Fn and VEGF immobilizing was reduced to Ra = 29.2 ± 2.45 nm, which was attributed to the fact that the biomolecules filled the pores of TiOHP surface during the fabrication process. This is an indication that heparin, Fn and VEGF exist in biofunctional coating.

### 3.1.3. Water contact angle

Surface hydrophilicity is a non-specific but sensitive method to validate the success of a surface modification. In this experiment, water contact angle of different sample surfaces was measured to assess the alteration of surface hydrophilicity during fabrication process. As shown in Fig. 3B, in comparison with pristine Ti, the water contact angle significantly decreased after NaOH activation and presented super-hydrophilicity, which was considered due to the synergy effect of abundant hydrophilic hydroxyl group (—OH) and capillary action of pore structure. Heparin and Fn were rich in hydrophilic groups, including hydroxyl, amine, carboxyl and sulfo group. Surface single immobilization with either heparin or Fn seems maintain the super-hydrophilic characteristic. However, the water contact angle was slightly increased on TiOHPHF and TiOHPHFV samples surface, which was considered maybe partly due to the exposure of hydrophobic groups caused by the interaction between heparin, Fn and VEGF. Compared with Ti, the Hep/Fn/VEGF biofunctional coating still was substantially more hydrophilic.

### 3.1.4. VEGF immunofluorescence staining

Immunofluorescence staining was used in this work to verify the presence of VEGF. VEGF appeared as green clusters on TiOHPHFV samples surface in Fig. 4, in contrast with the blank group, which showed no staining using the same procedure. Although the specific conformation of VEGF cannot be observed due to its nanoscale dimension, the immunofluorescence confirmed that VEGF was successfully immobilized on the materials surface.

## 3.2. Quantification of Hep/Fn/VEGF biofunctional coating

### 3.2.1. Quantification of heparin

The exposed heparin density on the samples surface was shown in Fig. 5A. NaOH activation caused a false positive heparin detection, which attributed to a non-specific adsorption of TBO to the micropore structure. The heparin density of TiOHPH sample, however, was significantly higher than the blank group of Ti (7.43 μg/cm$^2$ vs 0.99 μg/cm$^2$) and TiOH (7.43 μg/cm$^2$ vs 2.16 μg/cm$^2$), as well as the control group of TiOHPF (7.43 μg/cm$^2$ vs 1.02 μg/cm$^2$). The heparin density on TiOHPHF surface was slightly decreased compared with TiOHPH (6.53 μg/cm$^2$ vs 7.43 μg/cm$^2$), which was mainly attributed to charge neutralization of Fn to heparin. VEGF can also interact with heparin via its heparin binding domain, which thereby reduced the exposed heparin density on TiOHPHV surface further (5.89 μg/cm$^2$). In all, this result indicated that heparin was successfully immobilized on the materials surface, and presented a sufficient amount (much higher than 13.7 pmol/cm$^2$) to prevent thrombosis formation according to Byun et al. [47].

### 3.2.2. Semi-quantitative characterization of fibronectin

The amount of Fn on the samples surface was determined semiquantitatively by immunochemistry. As shown in Fig. 5B, compared to Ti, the TiOH samples exhibited slightly higher non-specific adsorption of the detection antibody, which also can be attributed to the microporous surface structure. On the Fn immobilized surfaces, TiOHPF, TiOHPHF and TiOHPHFV, Fn could be clearly detected by immunochemistry, confirming that Fn was successfully immobilized on the materials. However, due to the steric hindrance of heparin and VEGF to Fn during the fabrication, the exposed Fn

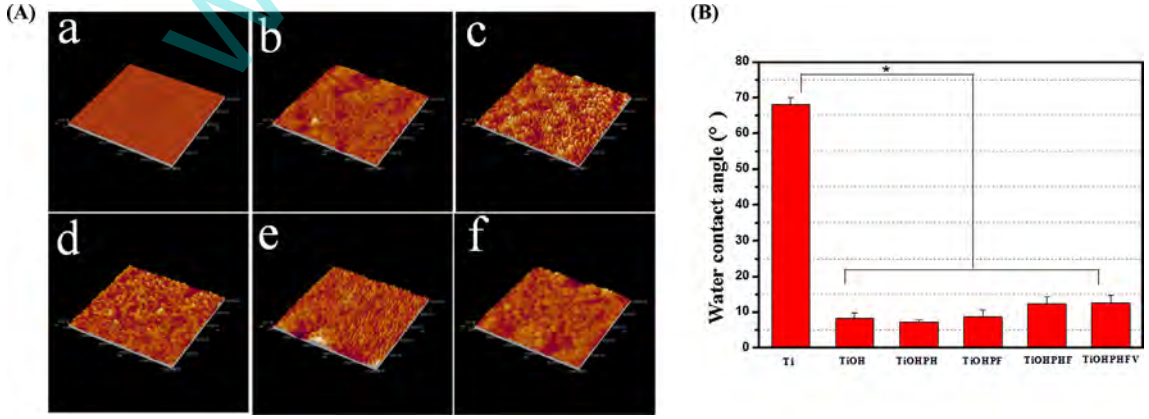


**Fig. 3.** (A) AFM morphology images of (a) pristine Ti; (b) TiOH; (c) TiOHPH; (d) TiOHPF; (e) TiOHPHF; (f) TiOHPHFV; (B) Water contact angle of different sample surfaces (mean ± SD, $N = 6$, $^*p < 0.05$).

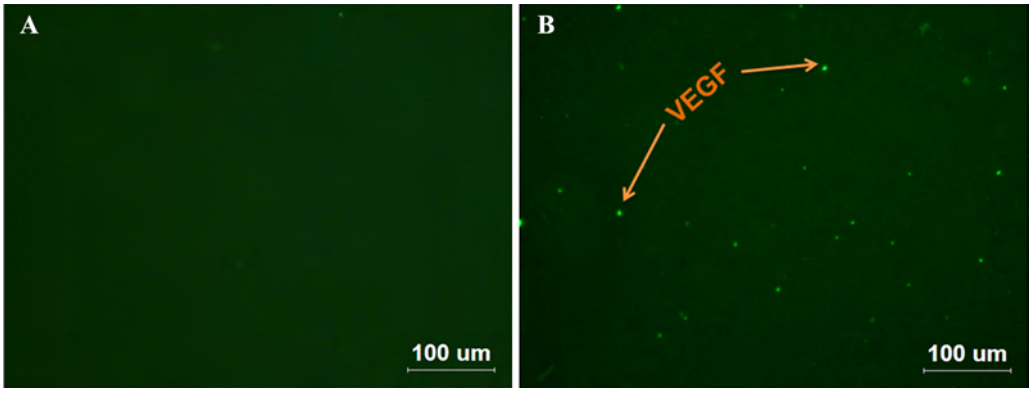


**Fig. 4.** VEGF immunofluorescence staining images of (A) TiOHPHF and (B) TiOHPHFV.

density was also slightly decreased on TiOHPHF and TiOHPHFV samples surface.

### 3.3. Hemocompatibility evaluation of Hep/Fn/VEGF biofunctional coating

#### 3.3.1. AT III binding

The anticoagulant effect of the Hep/Fn/VEGF biofunctional coating mainly depends on the interaction of heparin with AT III, which greatly accelerates the inactivation of thrombin. Thereby, the amount of absorbed AT III on different sample surfaces was determined to evaluate the anticoagulant potency of the biofunctional coating. As shown in Fig. 6, in comparison with the blank group of Ti and TiOH, the surface immobilized only with heparin significantly promoted the adsorption of AT III, whereas isolated Fn adsorption did not influence the AT III binding. Consistent with the determined heparin amount (Fig. 5A), the AT III binding on TiOHPHF and TiOHPHFV samples surface were slightly decreased compared with TiOHPH samples, attributed to the occupation of the AT III binding sequences of heparin by Fn and VEGF. But in total, the amount of absorbed AT III on TiOHPHFV samples surface was significantly enhanced compared to the blank control group. This provides the basis for an improved anticoagulant potential of the Hep/Fn/VEGF biofunctional coating.

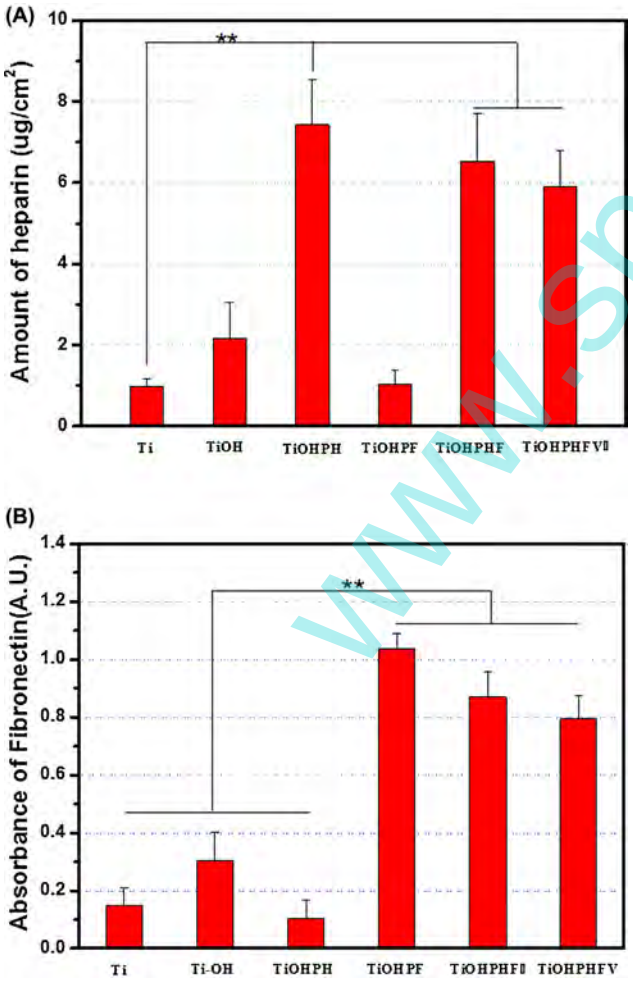


**Fig. 5.** (A) Amount of exposed heparin on the different sample surfaces; (B) Semi-quantitative characterization of exposed fibronectin on the different sample surfaces (mean ± SD, $N = 6$, $^{**}p < 0.01$).

#### 3.3.2. Clotting time

APTT, PT and TT were applied here to evaluate the anticoagulant potential of the surfaces in vitro. According to Fig. 7, the samples surface without heparin immobilization, including the blank group of Ti and TiOH and the control group of TiOHPF, presented no prolonged APTT, PT and TT values compared with plasma, which indicated that the NaOH activation and Fn immobilization have no influence on the clotting time. APTT was highly sensitive to heparin, and it was found that the APTT value of TiOHPH samples was prolonged by almost 45 s compared with PPP (Fig. 7A), while TT value prolonged about 4 s (Fig. 7B). Consistent with the AT III binding result (Fig. 6), the APTT values with TiOHPHF and TiOHPHFV were

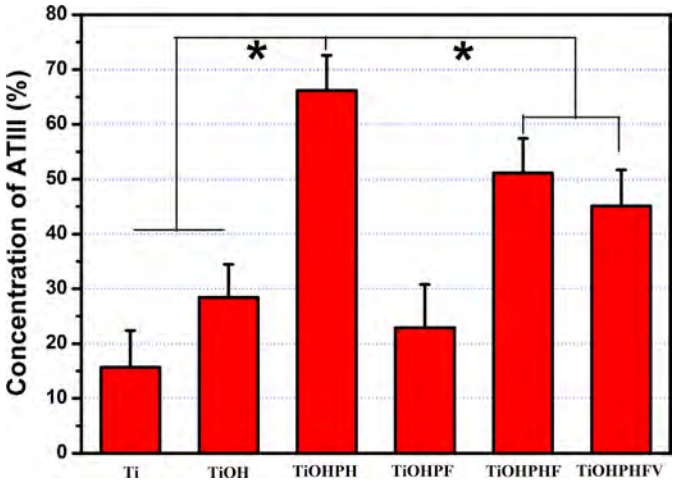


**Fig. 6.** Relative amount of AT III binding on different samples surface (mean ± SD, $N = 6$, $^{*}p < 0.05$ indicates significant difference compared with Ti and TiOH).

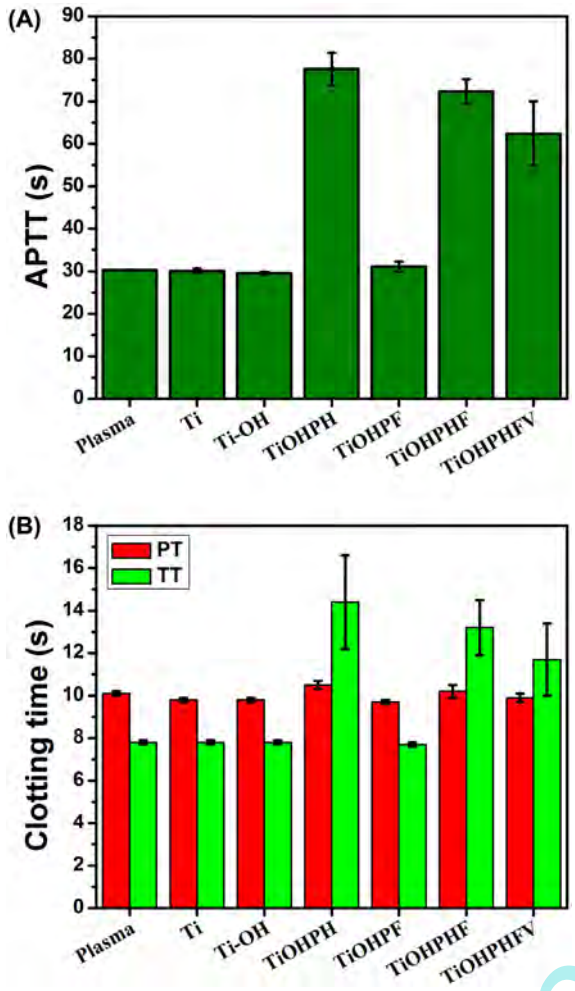


**Fig. 7.** Clotting time evaluation of different samples. (A) APTT result and (B) PT and TT result (mean ± SD, $N = 6$).

a bit lower than with the TiOHPH samples, but still exceeded the plasma values by more than 30 s (Fig. 7A), confirming the favorable anticoagulant property of the Hep/Fn/VEGF biofunctional coating. However, the heparinized surface seems has no significant influence on PT value (Fig. 7B), which may be partly due to the sensitivity of heparin to factor IXa was higher than IIa and XIa, though the exact mechanisms remain to be resolved.

### 3.3.3. Platelet adhesion and activation

For blood contacting biomaterials, activation of platelets and aggregate formation on materials surface may directly lead to thrombosis formation. Therefore, in vitro platelet adhesion and activation were tested here to further evaluate the hemocompatibility of the biofunctional coating, and the results are shown in Fig. 8. Fig. 8A shows the SEM images of platelets morphology on different sample surfaces. Obviously, large amounts of platelets aggregated on the blank Ti and TiOH surfaces, displaying dendritic or spreading dendritic morphology as sign of high activation. Immobilization of Fn only had no beneficial effect on the hemocompatibility, but seemed to promote platelet adhesion, as determined in the LDH assay (Fig. 8B), which was prepared for semi-quantitative evaluation of the amount of adherent platelets. On the heparin modified surface, including TiOHPH, TiOHPHF and TiOHPHFV, the density of adherent platelets was significantly decreased, and the cells mainly presented a round shape (Fig. 8A), indicating minor activation and favorable hemocompatibility. The result of LDH assay (Fig. 8B) further proved that the platelet adhesion was strongly reduced by the presence of heparin.

In addition, the platelet activation marker p-selectin on the various surfaces was determined. According to Fig. 8C, consistent with the SEM result, the heparin containing surfaces TiOHPH, TiOHPHF and TiOHPHFV, presented adequately inhibited platelet activation compared with the blanks and the control group TiOHPF. In total, the Hep/Fn/VEGF biofunctional coating presented a favorable antithrombotic property concerning plasmatic and platelet activation.

### 3.4. Cellular compatibility of the Hep/Fn/VEGF biofunctional coating

Endothelial progenitor cells (EPCs) are widely regarded to an important role in vascular endothelium injury healing and angiogenesis. Since the discovery of EPCs, the mechanism of endothelialization has been redefined based on the synergy action of ECs migration from the surrounding vascular tissue and EPCs homing from the bone marrow. Therefore, EPCs and ECs proliferation on the different samples was measured by cell counting and rhodamine 123 fluorescence staining to evaluate differences of cytocompatibility after the biofunctional modification.

Fig. 9 shows the cells counting and proliferation ratio results and fluorescence staining images of EPCs after incubation for 1 and 3 days. NaOH activation and isolated heparin immobilization had negative effect on EPCs adhesion and proliferation compared to bare Ti, which is mainly attributed to the high negatively charged characteristic of the TiOH surface and heparin. However, the immobilization of Fn improved EPCs adhesion and proliferation compared with TiOH, and the adherent cell density was comparable to that of Ti, as well as the cell projected area. On TiOHPHF surface, both the adherent density and proliferation ratio of EPCs were greatly increased in compared with TiOHPH and TiOHPF, this was considered partly due to the interaction of heparin and Fn, which may contribute to maintain Fn in its bioactive conformation and facilitate cellular adhesion and proliferation. In addition, VEGF significantly promoted the adhesion and proliferation of EPCs in compared with Ti ($^*p < 0.05$), confirming a favorable cytocompatibility of the Hep/Fn/VEGF coating for EPCs.

The result of ECs proliferation on the different surfaces is shown in Fig. 10. Similar to the EPCs growth tendency, the NaOH activation and heparin immobilization presented inhibitory effect on ECs growth, but the combination of heparin and Fn showed beneficial effect on ECs adhesion and proliferation. The existence of VEGF, however, showed no significant effect on ECs growth at day 1. But the cell density and proliferation ratio of ECs on TiOHPHFV samples at day 3 were significantly enhanced in compared with other groups ($^*p < 0.05$), and the adherent ECs presented the typical elliptical shape (Fig. 10) on TiOHPHFV, indicating that the Hep/Fn/VEGF coating could promote ECs spreading and proliferation.

## 4. Discussion

Implanted cardiovascular devices should inhibit thrombus formation and promote re-endothelialization simultaneously. Up to now, these requirements for the biocompatibility have been only partly achieved, and it is an ongoing challenge to obtain the ideal combination of surface chemistry and architecture to solve this problem. Surface modification with single molecules always lacks the ability for combined improvement of hemocompatibility and re-endothelialization after biomedical implantation. Therefore, a multifunctional microenvironment by combining specific biomolecules appears necessary to mimic the native microenvironment of the blood vessel wall. In the present study, heparin, Fn

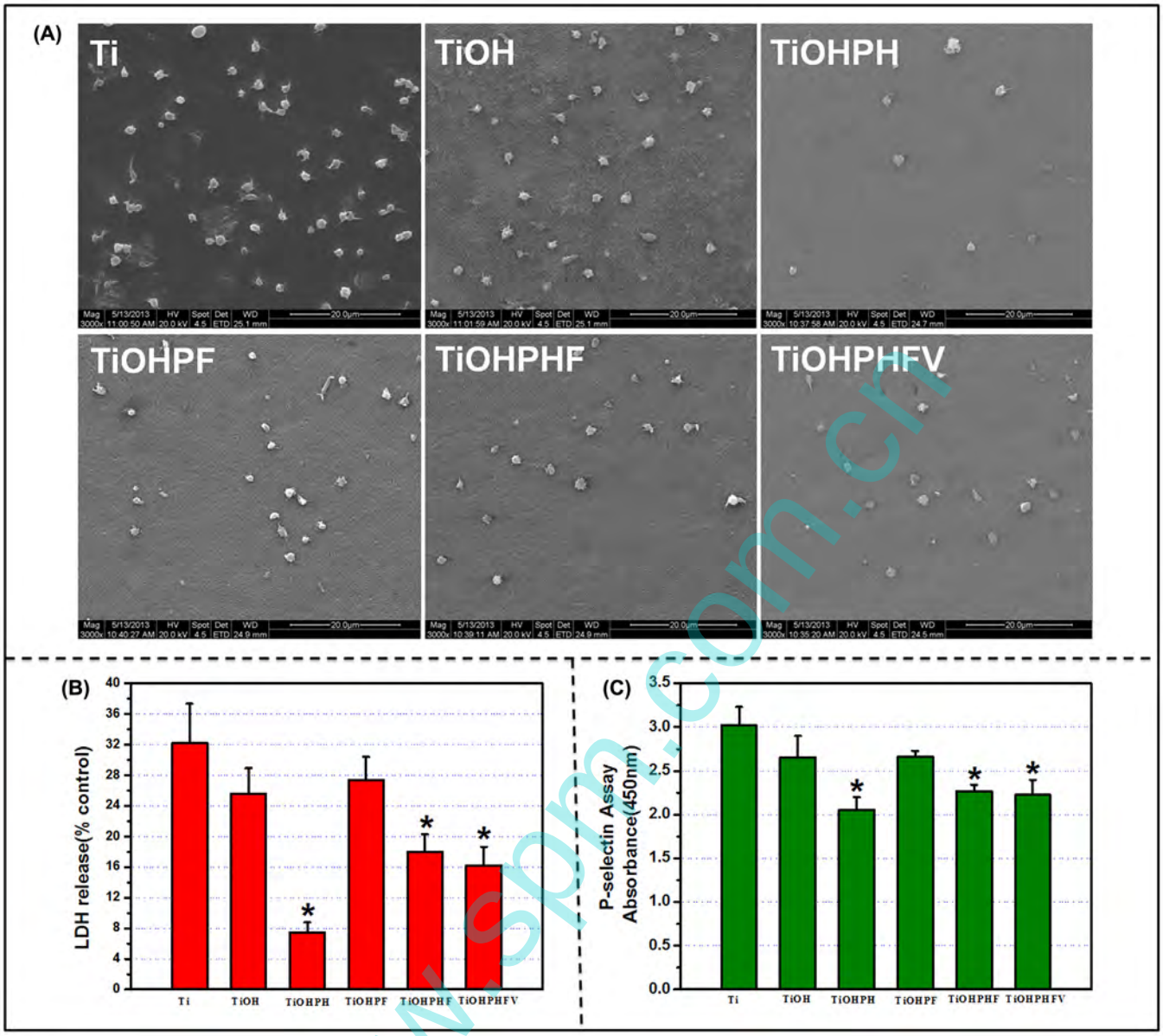


**Fig. 8.** (A) SEM images of adherent platelets on different samples surface; (B) semi-quantitative characterization of LDH release; (C) semi-quantitative characterization of p-selectin expression (mean ± SD, $N = 6$, $^{*}p < 0.05$ means significant difference in compared with Ti and TiOH).

and VEGF were immobilized on Ti surface. Heparin is an important anticoagulant which can strongly promote the AT III mediated inhibition of coagulation [32], it also has favorable pharmacologic effects in preventing inflammation and intimal hyperplasia. Fn, as an individual component of ECM, strongly promotes cell adhesion and migration, via interaction with integrins α5β1 and αvβ3, which are highly expressed on ECs and EPCs [37]. VEGF is another widely used cytokine in endothelium regeneration and angiogenesis, which can significantly improve ECs proliferation, survival and migration, as well as induce EPCs mobilization and differentiation to ECs. This study takes advantage of the specific interaction between Hep and Fn, and between Hep and VEGF for the formation of a Hep/Fn/VEGF biofunctional coating with the aim of promoting hemocompatibility and re-endothelialization simultaneously.

Fn is a heparin binding protein, besides, in acidic PBS solution (pH 4), Fn is positively charged and heparin is negatively charged, which may further facilitate the Hep/Fn complex formation. NaOH activation of Ti generates a negatively charged hydroxyl-rich surface, and thereby contributes to the electrostatic binding of positively charged PLL, which is amino-rich. Subsequently, the Hep/Fn complexes can bind to the amino-rich surface by electrostatic interaction. VEGF is also loaded on the surface via utilizing its specific interaction with heparin. The changes of the surface chemical composition during the fabrication were confirmed by XPS (Fig. 2), the presence of VEGF and Fn were further probed by immunochemistry and immunofluorescence (Figs. 4 and 5B), and heparin on the surface was verified using the electrostatic interaction with the dye TBO (Fig. 5A). Using these techniques, it could be confirmed that the biomolecules were successfully immobilized on the Ti surface, and the anti-coagulant and endothelialization stimulating property had to be analyzed.

### *4.1. Influence of the surface characters on the biocompatibility of the Hep/Fn/VEGF coating*

#### *4.1.1. Influence of the surface hydrophilicity*

Platelets and vascular cell attachment on a surface largely depend on the presence of adsorbed proteins from culture medium,

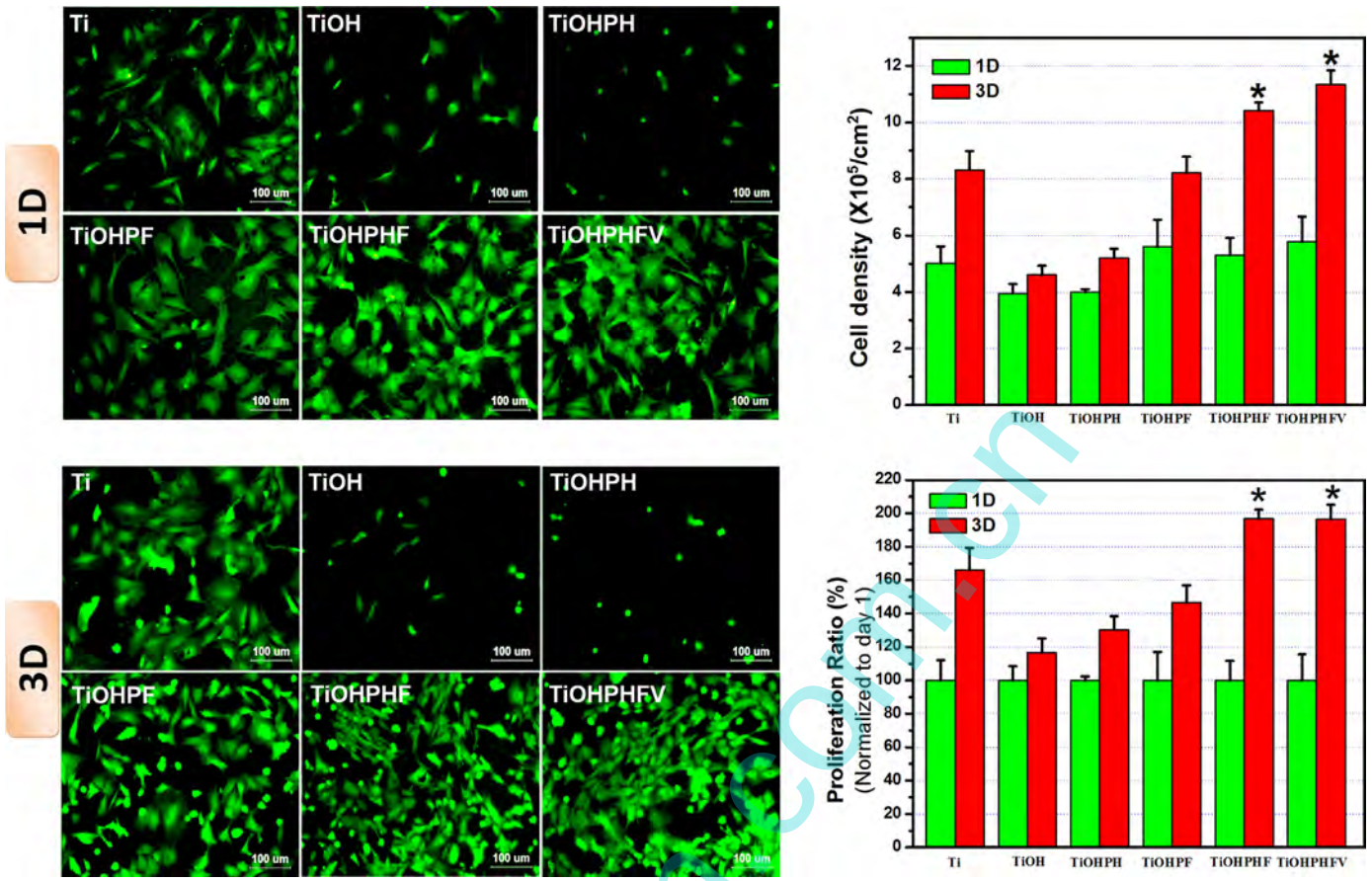


**Fig. 9.** EPCs fluorescence staining and cell counting result on different sample surfaces, the cell density at day 3 was normalized to day 1 to calculate the proliferation ratio (mean ± SD, $N = 6$, $^*p < 0.05$ means significant difference in compared with Ti and TiOH).

blood plasma or ECM components. The physical and chemical properties of the surface, such as chemical composition, hydrophilicity and topology, determine the composition and conformation of the adsorbed protein layers with impact on hemocompatibility and cellular behavior. Differences in surface hydrophilicity may trigger quantitative and qualitative variations in the absorbed proteins, generally, serum albumin is preferentially and strongly absorbed on hydrophobic surfaces, but adhesive proteins, such as Fn and Vn, are preferentially absorbed on hydrophilic surfaces [48]. As the cell membranes are hydrophilic, a hydrophilic material surface is suitable for cells adhesion and proliferation. However, very hydrophilic surfaces do not allow protein adsorption and cell adhesion any more. Thereby, increasing surface hydrophilicity in adequate range may be a way to direct platelets and vascular cells adhesion behavior. In this study, The NaOH activated surfaces was very hydrophilic and may contribute to preventing platelets adhesion and activation (Fig. 8), but also do harm to ECs and EPCs growth (Figs. 9 and 10). This phenomenon was partly attributed to the low protein adsorption on super-hydrophilic surface, and thereby specific adhesion ligands should be introduced to selectively inhibit platelets adhesion but has no harm to vascular cells growth.

#### 4.1.2. Influence of the surface roughness

Increasing the surface roughness also supports the adsorption of plasma proteins and thereby enhances the adhesion and survival of vascular cells. When cells contact with a material, intracellular kinase of signaling pathways are activated by interact with adsorbed adhesive proteins, and thereby promoting cells pseudopodia extension, and finally adhering on the material surface after morphologic changes. It has been reported that a porous surface structure can promote cells pseudopodia extension, enhancing the force between the cell layers and material surface [49]. Thus ECs can easily migrate and proliferate under the physiological flow shear stress, accelerating in situ endothelialization. However, extra surface roughness usually means larger area exposed to the platelets. Platelet adhesion and thrombogenesis accelerate when the surface roughness exceeds 50 nm [50], and a surface with micrometer-scale roughness induces more platelet adhesion early after exposure to blood [51]. However, Chung et al. [52] demonstrated that a surface roughness in the range of 10–100 nm also promotes ECs adhesion and proliferation. Therefore, it can be concluded that a surface roughness up to 50 nm may contribute to accelerated endothelium regeneration with reduced platelet adhesion. In all, proper surface roughness may promote endothelialization but not trigger thrombus formation. According to Table 2, the roughness of Hep/Fn/VEGF biofunctional coating increased in the desired range below 50 nm compared with Ti, which was considered may provide an adequate template for cell adhesion and growth (Table 3).

### 4.2. Influence of the biomolecules

Heparin is a glycosaminoglycan and presents the highest negative charge density of any known biological molecules, also known to exhibit different or even totally opposite function on regulating vascular cells behaviors in different setup [53–55]. The over dosage of heparin on cardiovascular devices may delay endothelium regeneration and raise the risk of late thrombotic events. In contrast, Fn can strongly promote ECs adhesion, proliferation and migration, and may compensate for the adverse effects of heparin to

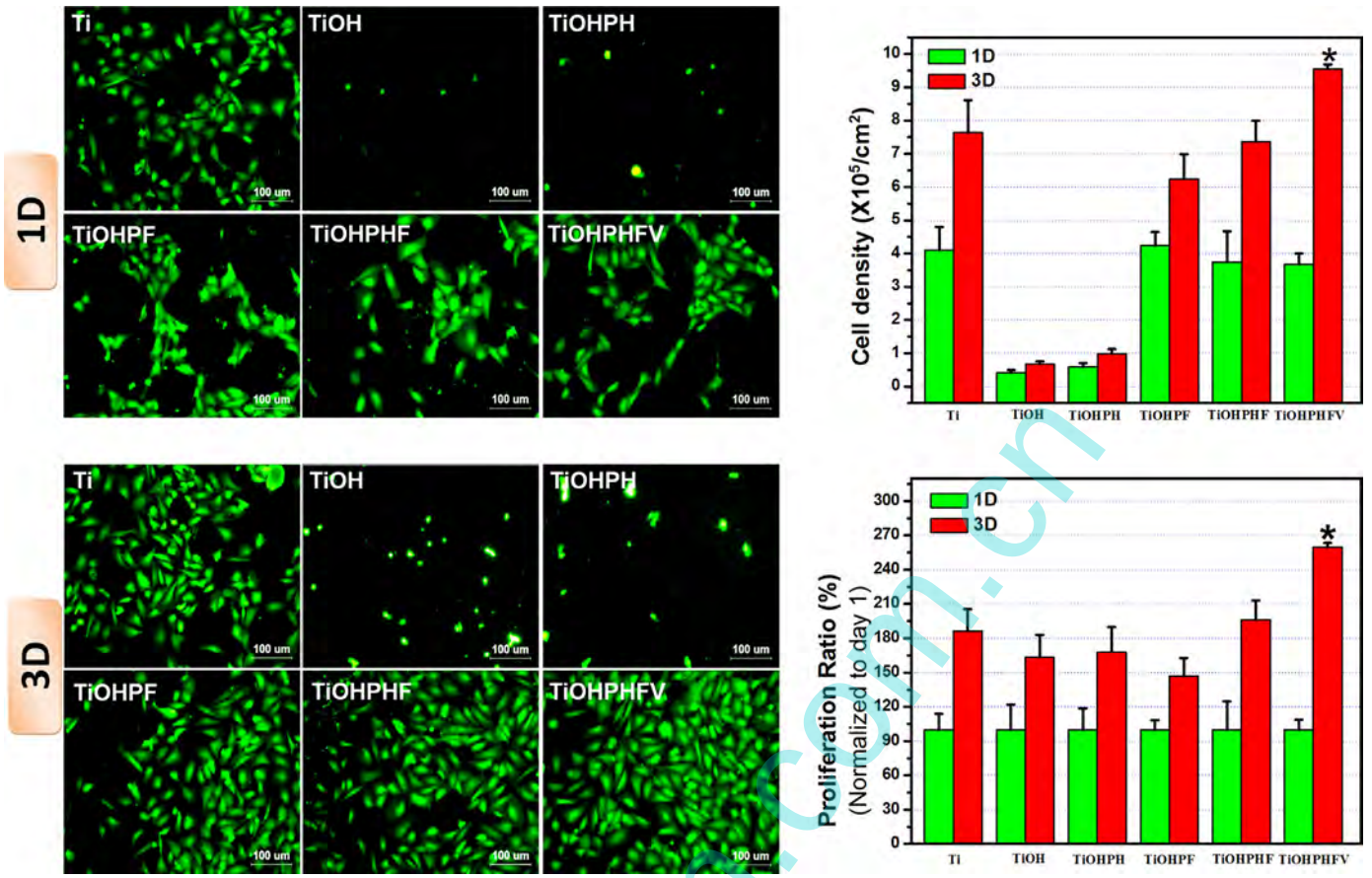


**Fig. 10.** ECs fluorescence staining and cell counting result on different sample surfaces, the cell density at day 3 was normalized to day 1 to calculate the proliferation ratio (mean ± SD, $N = 6$, $^*p < 0.05$ means significant difference in compared with Ti and TiOH).

ECs. However, Fn also stimulates platelet adhesion and aggregation through their integrin aIIbβ3 receptors [37]. Therefore the surface binding density of heparin and Fn should be probably adjusted. We previously optimized the coating protocol for this aspect [38] and applied this also here. In addition, VEGF got introduced to further promote the endothelialization of the modified surface. Although VEGF in the coating slightly decreased the AT III binding (Fig. 6) and clotting time (Fig. 7), number and activation degree of adherent platelets on the Hep/Fn/VEGF coating was significantly decreased compared with Ti and TiOH samples (Fig. 8), indicating that the biofunctional coating provided an excellent anticoagulant property to the Ti material.

Besides providing superior hemocompatibility, implanted cardiovascular devices must facilitate rapid endothelialization. As described, however, heparinized surfaces are always considered to suppress ECs adhesion and proliferation due to insufficient cellular binding sites and their high negative charge characteristic. In this study, this is circumvented, because Fn and VEGF introduce abundant binding sites for the interaction with ECs and EPCs. According to Figs. 9 and 10, NaOH treated Ti inhibited ECs and EPCs adhesion and proliferation, and the surface with only heparin immobilized also did not show any beneficial effect on EPCs and ECs adhesion, but the cells present shrinkage morphology on the TiOHPH surface. In contrast, the Hep/Fn immobilized surface significantly promoted EPCs and ECs adhesion and proliferation, and the introduction of VEGF further improved the growth profile.

Fn as a promoting vascular cells adhesion biomacromolecule, forms complexes with heparin by specific interaction with the heparin binding sites. VEGF also has heparin binding sites for specific interaction with heparin. In the Hep/Fn/VEGF biofunctional coating, heparin and Fn cross twisting with each other and VEGF distributes irregularly in this Hep/Fn complex, achieving balance by mutual competitive adsorption. Therefore, each biomolecule is subject to steric hindrance from other biomolecules, which may lead to shielding and consumption of some biological active sites. However, obviously, despite shielding the molecules still exhibit sufficient bioactivity for the desired blood compatibility. The exposed heparin exhibits preferable hemocompatibility by interaction with AT III (Fig. 8); Fn can significantly promote vascular cell adhesion and proliferation by its RGD cellular binding sites (Figs. 9 and 10); and VEGF promotes EPCs and ECs adhesion and proliferation (Figs. 9 and 10), contributing to re-endothelialization. In total, the Hep/Fn/VEGF coating exhibits preferable hemocompatibility and capability for endothelialization, providing an EPC homing microenvironment for in situ endothelialization.

**Table 3**
Roughness of different samples surface determined by AFM.

| | Ti | TiOH | TiOHPH | TiOHPF | TiOHPHF | TiOHPHFV |
|---|---|---|---|---|---|---|
| Sa (nm) | 3.65 ± 0.27 | 38 ± 1.51 | 34.5 ± 0.56 | 30 ± 0.98 | 31.9 ± 0.76 | 29.2 ± 2.45 |
| Sq (nm) | 3.72 ± 0.63 | 41.2 ± 0.65 | 41.2 ± 0.65 | 33.9 ± 1.09 | 33.8 ± 1.83 | 31 ± 4.68 |

Proper combination of physicochemical and biological surface properties is necessary for improving the biocompatibility of cardiovascular devices. This can be achieved by multifunctional surface modification based on specific biomolecules. This study takes advantage of the intermolecular interactions between the biomolecules, heparin, Fn and VEGF for their immobilization on a Ti surface. The bioactivity of different biomolecules was well retained and the biocompatibility of biofunctional coating was proved excellent. Further investigation will focus on the biocompatibility evaluation of the Hep/Fn/VEGF biofunctional coating by in vitro induced-endothelialization studies and in vivo animal experiments.

## 5. Conclusion

The major challenge in the biocompatible design of stent surfaces faced today is the conflict of hemocompatibility and stimulation of endothelialization at the same time. Some anticoagulant molecules prevent re-endothelialization, whereas a few endothelialization promoting molecules deteriorate hemocompatibility. In the present work, a multifunctional microenvironment was constructed on Ti surface by heparin, fibronectin and VEGF to support induced endothelialization. XPS, toluidine blue O binding and immunochemistry results demonstrated that all biomolecules were immobilized successfully on an activated Ti surface, constructing the Hep/Fn/VEGF biofunctional coating. The surface roughness and water contact angle measurement stated that the Hep/Fn/VEGF biofunctional coating was smoother and more hydrophilic than the native Ti surface. In hemocompatibility evaluation, higher AT III binding density, prolonged APTT values, less platelet activation and aggregation were exhibited on the Hep/Fn/VEGF biofunctional coating compared with Ti. The Hep/Fn/VEGF biofunctional coating significantly promotes EPCs and ECs attachment, spreading and proliferation, maintaining favorable biological activity. Besides, influence of the surface characters and biomolecules interaction on the Hep/Fn/VEGF biocompatibility was analyzed in this work. It was demonstrated that the suitable surface hydrophilicity and proper surface roughness were beneficial to promote anticoagulant and re-endothelial performance of biomaterials. The Hep/Fn/VEGF biofunctional coating maintained favorable hemocompatibility and promoted the re-endothelialization simultaneously. This method can be extended to other biomolecule immobilization on different biomaterials to obtain diverse biofunction. It is possible to immobilize biomolecules with different functions on an implant surface to construct a biomimetic microenvironment by competing and balancing between biomolecules. Taking advantage of each molecule, a desired functional microenvironment can be obtained. Therefore, this work provides a promising approach to mimic native biological microenvironment for implantation devices to obtain desired long-term biocompatibility.

## Acknowledgements

The authors gratefully acknowledge the financial support of the Key Basic Research Program (2011CB606204), National Natural Science Foundation of China (No. 31170916#, No. 31470921# and No. 31470926#), and the Fundamental Research Funds for the Central Universities (No. SWJTU11ZT11).

## References

[1] K.A. Fox, S.G. Goodman, W. Klein, D. Brieger, P.G. Steg, O. Dabbous, A. Avezum, Management of acute coronary syndromes. Variations in practice and outcome: findings from the Global Registry of Acute Coronary Events, Eur. Heart J. 23 (2002) 1177–1189.
[2] D. Hasdai, S. Behar, L. Wallentin, N. Danchin, A.K. Gitt, E. Boersma, P.M. Fioretti, M.L. Simoons, A. Battler, A prospective survey of the characteristics, treatments and outcomes of patients with acute coronary syndromes in Europe and the Mediterranean basin: the Euro Heart Survey of acute coronary syndromes, Eur. Heart J. 23 (2002) 1190–2001.
[3] F.D. Pagani, L.W. Miller, S.D. Russell, K.D. Aaronson, R. John, A.J. Boyle, J.V. Conte, R.C. Bogaev, T.E. MacGillivray, Y. Naka, D. Mancini, H.T. Massey, L. Chen, C.T. Klodell, J.M. Aranda, N. Moazami, G.A. Ewald, D.J. Farrar, O.H. Frazier, Extended mechanical circulatory support with a continuous-flow rotary left ventricular assist device, J. Am. Coll. Cardiol. 54 (2009) 312–321.
[4] M. Schillinger, S. Sabeti, P. Dick, J. Amighi, W. Mlekusch, O. Schlager, C. Loewe, M. Cejna, J. Lammer, E. Minar, Sustained benefit at two years of primary femoropopliteal stenting compared with balloon angioplasty with optional stenting, Circulation 115 (2007) 2745–2749.
[5] H.E. Achneck, R.M. Jamiolkowski, A.E. Jantzen, J.M. Haseltine, W.O. Lane, J.K. Huang, L.J. Galinat, M.J. Serpe, F.H. Lin, M. Li, A. Parikh, L. Ma, T. Chen, B. Sileshi, C.A. Milano, C.S. Wallace, T.V. Stabler, J.D. Allen, G.A. Truskey, J.H. Lawson, The biocompatibility of titanium cardiovascular devices seeded with autologous blood-derived endothelial progenitor cells: EPC-seeded antithrombotic Ti Implants, Biomaterials 32 (2011) 10–18.
[6] L. Mauri, T.S. Silbaugh, R.E. Wolf, K. Zelevinsky, A. Lovett, Z. Zhou, F.S. Resnic, S.L. Normand, Long-term clinical outcomes after drug-eluting and bare-metal stenting in Massachusetts, Circulation 118 (2008) 1817–1827.
[7] H.C. Lowe, S.N. Oesterle, L.M. Khachigian, Coronary in-stent restenosis: current status and future strategies, J. Am. Coll. Cardiol. 39 (2002) 183–193.
[8] R.S. Schwartz, Animal models of human coronary restenosis, in: E.J. Topol (Ed.), Textbook of Interventional Cardiology, 2nd ed., W.B. Saunders, Philadelphia, PA, 1994, pp. 365–381.
[9] G.S. Mintz, J.J. Popma, A.D. Pichard, K.M. Kent, L.F. Satler, C. Wong, M.K. Hong, J.A. Kovach, M.B. Leon, Arterial remodelling after coronary angioplasty: a serial intravascular ultrasound study, Circulation 94 (1996) 35–43.
[10] X.H. Wang, B. Jia, Z.G. Chen, K.Q. Wang, Study on inducing of cord blood derived endothelial progenitor cells into endothelial cells, J. Appl. Clin. Pediatr. 21 (2006) 1407–1409.
[11] P. Zhang, J.X. Wu, B. Leng, Research progress of endothelial progenitor cells and endothelializaiton after PTCA, Chin. Heart J. 23 (2011) 535–537.
[12] Q. Shao, C.Q. Wand, H.H. Fan, M. Jiang, Y. Liu, X.X. Nie, L. Gao, Inducing cord blood and peripheral blood derived EPCs into endothelial cells in vitro, Chin. Heart J. 18 (2006) 18–22.
[13] H.C. Cheng, S.Y. Chiou, C.M. Liu, M.H. Lin, C.C. Chen, K.L. Ou, Effect of plasma energy on enhancing biocompatibility and hemocompatibility of diamond-like carbon film with various titanium concentrations, J. Alloy Compd. 477 (2009) 931–935.
[14] W.E. Yang, H.H. Huang, Improving the biocompatibility of titanium surface through formation of a $TiO_2$ nano-mesh layer, Thin Solid Films 518 (2010) 7545–7550.
[15] K. Enomoto, T. Hasebe, R. Asakaw, A. Kamijo, Y. Yoshimoto, T. Suzuki, K. Takahashi, A. Hotta, Controlling the drug release rate from biocompatible polymers with micro-patterned diamond-like carbon (DLC) coating, Diam. Relat. Mater. 19 (2010) 806–813.
[16] X. Sun, Z. Cao, C.K. Yeh, Y. Sun, Antifungal activity, biofilm-controlling effect, and biocompatibility of poly(N-vinyl-2-pyrrolidinone)-grafted denture materials, Colloids Surf. B: Biointerfaces 110 (2013) 96–104.
[17] M. Abdel-Hady Gepreel, M. Niinomi, Biocompatibility of Ti-alloys for long-term implantation, J. Mech. Behav. Biomed. Mater. 20 (2013) 407–415.
[18] R.A. Hoshi, R. Van Lith, M.C. Jen, J.B. Allen, K.A. Lapidos, G. Ameer, The blood and vascular cell compatibility of heparin-modified ePTFE vascular grafts, Biomaterials 34 (2013) 30–41.
[19] S. Schwarz, S.M. Ponce-Vargas, A. Licea-Claverie, C. Steinbach, Chitosan and mixtures with aqueous biocompatible temperature sensitive polymer as flocculants, Colloids. Surf. A: Physicochem. Eng. Asp. 413 (2012) 7–12.
[20] K.A. McKenna, M.T. Hinds, R.C. Sarao, P.C. Wu, C.L. Maslen, R.W. Glanville, D. Babcock, K.W. Gregory, Mechanical property characterization of electrospun recombinant human tropoelastin for vascular graft biomaterials, Acta Biomater. 8 (2012) 225–233.
[21] X. Wang, C. Yan, K. Ye, Y. He, Z.H. Li, J.D. Ding, Effect of RGD nanospacing on differentiation of stem cells, Biomaterials 34 (2013) 2865–2874.
[22] Q.L. Li, N. Huang, C. Chen, J.L. Chen, K.Q. Xiong, J.Y. Chen, T.X. You, J. Jin, X. Liang, Oriented immobilization of anti-CD34 antibody on titanium surface for self-endothelialization induction, J. Biomed. Mater. Res. A 94A (2010) 1283–1293.
[23] C.H. Wang, T.M. Wang, T.H. Young, Y.K. Lai, M.L. Yen, The critical role of ECM proteins within the human MSC niche in endothelial differentiation, Biomaterials 34 (2013) 4223–4234.
[24] I. d'Angelo, O. Oliviero, F. Ungaro, F. Quaglia, P.A. Netti, Engineering strategies to control vascular endothelial growth factor stability and levels in a collagen matrix for angiogenesis: the role of heparin sodium salt and the PLGA-based microsphere approach, Acta Biomater. 9 (2013) 7389–7398.
[25] A. Zhu, M. Zhang, J. Wu, J. Shen, Covalent immobilization of chitosan/heparin mixture with a photosensitive hetero-bifunctional crosslinking reagent on PLA surface, Biomaterials 23 (2002) 4657–4665.
[26] Z. Yang, J. Wang, R. Luo, M.F. Maitz, F. Jing, H. Sun, N. Huang, The covalent immobilization of heparin to pulsed-plasma polymeric allylamine films on 316L stainless steel and the resulting effects on hemocompatibility, Biomaterials 31 (2010) 2072–2083.
[27] D. Guarnieri, A. De Capua, M. Ventre, A. Borzacchiello, C. Pedone, D. Marasco, M. Ruvo, P.A. Netti, Covalently immobilized RGD gradient on PEG hydrogel

scaffold influences cell migration parameters, Acta Biomater. 6 (2010) 2532–2539.
[28] T.P. Cooper, M.V. Sefton, Fibronectin coating of collagen modules increases in vivo HUVEC survival and vessel formation in SCID mice, Acta Biomater. 7 (2011) 1072–1083.
[29] X. Wang, X. Zhang, J. Castellot, I. Herman, M. Iafrati, D.L. Kaplan, Controlled release from multilayer silk biomaterial coatings to modulate vascular cell responses, Biomaterials 29 (2008) 894–903.
[30] S. Meng, Z. Liu, L. Shen, Z. Guo, L.L. Chou, W. Zhong, Q. Du, J. Ge, The effect of a layer-by-layer chitosan-heparin coating on the endothelialization and coagulation properties of a coronary stent system, Biomaterials 30 (2009) 2276–2287.
[31] G.F. Pineo, R.D. Hull, 5 Heparin and low-molecular-weight heparin in the treatment of venous thromboembolism, Baillières Clin. Haematol. 11 (1998) 621–637.
[32] P.S. Damus, M. Hicks, R.B. Rosenberg, Anticoagulant action of heparin, Nature 246 (1997) 355–357.
[33] E.M. Stewart, X. Liu, G.M. Clark, R.M. Kapsa, G.G. Wallace, Inhibition of smooth muscle cell adhesion and proliferation on heparin-doped polypyrrole, Acta Biomater. 8 (2012) 194–200.
[34] S.C. Thornton, S.N. Mueller, E.M. Levine, Human endothelial cells: use of heparin in cloning and long-term serial cultivation, Science 222 (1983) 623–625.
[35] R. Pankov, K.M. Yamada, Fibronectin at a glance, J. Cell. Sci. 115 (2002) 3861–3863.
[36] S. Astrof, R.O. Hynes, Fibronectins in vascular morphogenesis, Angiogenesis 12 (2009) 165–175.
[37] J. Cho, D.F. Mosher, Enhancement of thrombogenesis by plasma fibronectin cross-linked to fibrin and assembled in platelet thrombi, Blood 107 (2006) 3555–3563.
[38] G. Li, P. Yang, W. Qin, M.F. Maitz, S. Zhou, N. Huang, The effect of coimmobilizing heparin and fibronectin on titanium on hemocompatibility and endothelialization, Biomaterials 32 (2011) 4691–4703.
[39] G. Li, F. Zhang, Y. Liao, P. Yang, N. Huang, Coimmobilization of heparin/fibronectin mixture on titanium surfaces and their blood compatibility, Colloids Surf. B: Biointerfaces 81 (2010) 255–262.
[40] T. Boontheekul, D.J. Mooney, Protein-based signaling systems in tissue engineering, Curr. Opin. Biotechnol. 14 (2003) 559–565.
[41] C.K. Poh, Z. Shi, T.Y. Lim, K.G. Neoh, W. Wang, The effect of VEGF functionalization of titanium on endothelial cells in vitro, Biomaterials 31 (2010) 1578–1585.
[42] J.L. Zhou, M.H. Zou, Y.C. Chen, C. Zhou, J.W. Shi, N.G. Dong, Co-culture, proliferation and migration of human umbilical cord blood-derived endothelial progenitor cells with vascular endothelial growth factor and basic fibroblast growth factor, J. Clin. Rehabil. Tissue Eng. Res. 15 (2011) 1000–1004.
[43] S.M. Anderson, T.T. Chen, M.L. Iruela-Arispe, T. Segura, The phosphorylation of vascular endothelial growth factor receptor-2 (VEGFR-2) by engineered surfaces with electrostatically or covalently immobilized VEGF, Biomaterials 30 (2009) 4618–4628.
[44] T. Liu, Y. Liu, Y. Chen, S. Liu, M. Maitz, X. Wang, K. Zhang, J. Wang, Y. Wang, J. Chen, N. Huang, Immobilization of heparin/poly-l-lysine nanoparticles on dopamine coated surface to construct heparin density gradient for selective direction of platelet and vascular cell behavior, Acta Biomater. (2013), http://dx.doi.org/10.1016/j.actbio.2013.12.013.
[45] Y.H. Shen, M.S. Shoichet, M. Radisic, Vascular endothelial growth factor immobilized in collagen scaffold promotes penetration and proliferation of endothelial cells, Acta Biomater. 4 (2008) 477–489.
[46] K. Zhang, J.A. Li, K. Deng, T. Liu, J.Y. Chen, N. Huang, The endothelialization and hemocompatibility of the functional multilayer on titanium surface constructed with type IV collagen and heparin, Colloids Surf. B: Biointerfaces 108 (2013) 295–304.
[47] Y. Byun, H.A. Jacobs, J. Feijen, S.W. Kim, Effect of fibronectin on the binding of antithrombin III to immobilized heparin, J. Biomed. Mater. Res. 30 (1996) 95–100.
[48] E. Monchaux, P. Vermette, Effects of surface properties and bioactivation of biomaterials on endothelial cells, Front. Biosci. 2 (2010) 239–255.
[49] J.A. Beamish, L.C. Geyer, N.A. Haq-Siddiqi, K. Kottke-Marchant, R.E. Marchant, The effects of heparin releasing hydrogels on vascular smooth muscle cell phenotype, Biomaterials 30 (2009) 6286–6294.
[50] Q. Liu, X.N. Cheng, H.X. Fei, Effect of micromagnetic field surface roughness of 316L stainless steel and NiTi alloy on blood compatibility, Med. Biol. Eng. Comput 49 (2011) 359–364.
[51] J.Y. Park, C.H. Gemmell, J.E. Davies, Platelet interactions with titanium: modulation of platelet activity by surface topography, Biomaterials 22 (2001) 2671–2682.
[52] T.W. Chung, D.Z. Liu, S.Y. Wang, S.S. Wang, Enhancement of the growth of human endothelial cells by surface roughness at nanometer scale, Biomaterials. 24 (2003) 4655–4661.
[53] R. Cariou, J.L. Harousseau, G. Tobelem, Inhibition of human endothelial cell proliferation by heparin and steroids, Cell, Biol. Int. Rep. 12 (1988) 1037–1047.
[54] A.A. Khorana, A. Sahni, O.D. Altland, C.W. Francis, Heparin inhibition of endothelial cell proliferation and organization is dependent on molecular weight, Arterioscler. Thromb. Vasc. Biol. 23 (2003) 2110–2115.
[55] C.J. Bettinger, B. Orrick, A. Misra, R. Langer, J.T. Borenstein, Microfabrication of poly (glycerol-sebacate) for contact guidance applications, Biomaterials. 27 (2006) 2558–2565.